This article has been accepted for publication in IEEE/ASME Transactions on Mechatronics. This is the author's version which has not been fully edited and content may change prior to final publication. Citation information: DOI 10.1109/TMECH.2022.3219108

Dynamic Capture Using a Trap-like Soft Gripper with Stiffness Anisotropy

Shangkui Yang, Yongxiang Zhou, Ian D. Walker, *Fellow, IEEE*, Chenghao Yang, David T. Branson III, Zhibin Song, *Member, IEEE,* Jian S. Dai, *Fellow, IEEE,* Rongjie Kang*

***Abstract*—Dynamic capture is a common skill that humans have practiced extensively but is a challenging task for robots in which sensing, planning and actuation must be tightly coordinated to deal with targets of diverse shapes, sizes, and velocity. In particular, the impact force may cause serious damage to a rigid gripper and even its carrier, e.g., a robotic arm. Existing soft grippers suffer from low speed and force to actively respond to capturing dynamic targets. In this paper, we propose a soft gripper capable of efficient capture of dynamic targets, taking inspiration from the biological structures of multi tentacled animals or plants. The presented gripper uses a cluster of tentacles to achieve an omni-directional envelope and high tolerance to dynamic target during the capturing process. In addition, a stiffness anisotropy property is implemented to the tentacle structure to form a 'trap' making it easy for the targets to enter yet difficult to escape. We also present an analytical model for the tentacle structure to describe its deformation during the collision with a target. In experiments, we construct a robotic prototype and demonstrate its ability to capture dynamic targets.**

***Index Terms*—Dynamic capture, Soft gripper, Tentacle cluster, Stiffness anisotropy.**

I. Introduction

A well trained human is able to catch dynamic targets traveling in the air or water (e.g., a baseball or a fish) through real-time coordination between eyes and muscles that allows for highly skillful moves [1]. However, this task is particularly challenging for robotic systems because accurate sensing, planning, and responding should be completed in a very short period of time [2, 3]. This paper proposes a new design of bio-inspired robotic gripper to reduce these challenges.

Previous works on dynamic capture employed a rigid gripper mounted on a robotic arm tip to grasp targets [4, 5]. This method has the advantages of good repeatability and high strength. However, it needs to identify the trajectory and posture of the dynamic targets rapidly, and requires accurate actuation of the rigid gripper [6]. Such a strategy will generate enormous impact forces, which may cause targets to bounce out of the gripper before being enveloped. In addition, the huge impact may damage the robot and target [7].

During the capture process using rigid grippers, it is important to implement active control on the robotic arm and gripper to provide synchronous movement and compliance between the gripper and target. Kim *et al.* presented a synchronous motion planning method to capture irregular dynamic targets through a machine learning algorithm [8]. This method was later improved by Salehian *et al.*, using a linear parameter varying strategy to control the robot to reach and follow the target, and therefore exhibiting some 'compliance' [9]. Furthermore, impedance control methods were utilized to absorb the impact of the dynamic target, and maintain stability during the collision [10]. In recent works, the effects of impact forces were modeled as state-dependent uncertainties, and the robust locomotion of robotic systems under uncertainties has been achieved by using adaptive artificial time delay control and improved adaptive sliding mode control [11, 12].

The above methods are highly dependent on active control algorithms that require high-performance control hardware, e.g., high-speed sensors and actuators. In recent years, the fast development of compliant, or even soft mechanisms provides a new way to achieve tolerant manipulation, making use of the redundant degrees-of-freedom (DOF) and reducing the demand for active control [13]. Moreover, the intrinsic compliance can increase adaptability and safety of the gripper. Wang *et al.* presented a statically balanced gripper to provide a constant grasping force to manipulate objects of various sizes through compliant mechanisms [14]. Odhner *et al.* presented a compliant underactuated fingers that are capable of both firm power grasps and low-stiffness fingertip grasps [15]. Sinatra *et al.* designed a soft gripper for ultra-gentle capture of marine organisms [16]. Alici *et al.* presented a 3-D printed soft gripper equipped with three fingers and a suction cup, which is able to pick and place wide variety of objects [17]. Besides

This work was supported by the Natural Science Foundation of China (Grant No. 51875393), and the National Key R&D Program of China (Grant No. 2018YFB1304600, No. 2019YFB1309800). (*Corresponding author: Rongjie Kang*.)

Shangkui Yang is with the Key Laboratory of Mechanism Theory and Equipment Design of Ministry of Education School of Mechanical Engineering, Tianjin University, Tianjin 300072, China (e-mail: yangshangkui@tju.edu.cn)

Yongxiang Zhou, Chenghao Yang and Zhibin Song are with the Key Laboratory of Mechanism Theory and Equipment Design of Ministry of Education School of Mechanical Engineering, Tianjin University, Tianjin 300072, China (e-mail: zhouyx@tju.edu.cn; chenghao.yang@outlook.com; songzhibin@tju.edu.cn)

Ian D. Walker is with the Department of Electrical and Computer Engineering, Clemson University, Clemson SC 29634, USA (e-mail: iwalker@clemson.edu).

D.T. Branson is with the Advanced Manufacturing Technology Research Group, Faculty of Engineering, University of Nottingham, Nottingham NG7 2RD, UK (email: David.Branson@nottingham.ac.uk).

Jian S. Dai is with the Institute for Robotics, Southern University of Science and Technology, Shenzhen, China, and also with the Centre for Robotics Research, King's College London, WC2R 2LS London, U.K. (e-mail: jian.dai@kcl.ac.uk)

Rongjie Kang is with the Key Laboratory of Mechanism Theory and Equipment Design of Ministry of Education School of Mechanical Engineering, Tianjin University, Tianjin 300072, China (e-mail: rjkang@tju.edu.cn)

This article has been accepted for publication in IEEE/ASME Transactions on Mechatronics. This is the author's version which has not been fully edited and content may change prior to final publication. Citation information: DOI 10.1109/TMECH.2022.3219108

compliance, strength is also an important factor when dealing with dynamic targets with high kinetic energy, and is a main limitation of existing compliant/soft robotic grippers. Although there have been many studies on tuning stiffness for soft actuators, [18, 19] the output force and response time cannot generally meet the requirements for capturing dynamic targets [20].

The key point to capturing dynamic targets is how to combine strength with flexibility to achieve fast response and high adaptability, while reducing the demand for active control that may be costly and time consuming. There are some impressive cases in nature, including animals and plants [21, 22]. Sea anemone stand still under the sea and use a cluster of tentacles to capture fish moving in various directions. Drosera use multi-tentacles to form an arc-shaped 'trap' to envelop insects. They have very limited maneuvering ability, yet they are able to capture fast moving prey, with the help of a cluster of tentacles, as shown in **Fig.** 1(a)(b). This tentacle cluster-based capture mechanism does not rely on the precise control of a single tentacle, but rather on cooperation between the tentacles to intercept dynamic targets in various directions, showing excellent tolerance. As long as the prey enters the tentacle cluster, it will be retarded and eventually enveloped by the tentacles. Meanwhile, we note that some plants in nature, e.g., Mimosa, [23] can fold their leaves quickly in one direction while generating considerable stiffness in the reverse direction to maintain the folded structure, [24] as shown in **Fig.** 1(c). If this anisotropic stiffness feature can be applied to a robotic gripper for capturing dynamic targets, it will be possible to achieve soft contact with the target in one direction, while maintaining a strong grasp in the opposite direction. Although this anisotropic stiffness can be achieved via active control, we believe a passive mechanism will be more suitable for dynamic capture where fast and reliable responses are required.

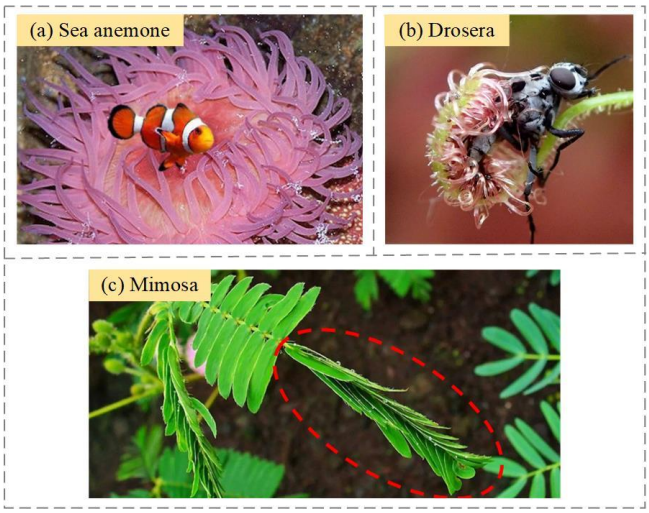

Fig. 1. Multi-tentacle capturing behavior and anisotropic stiffness in nature: (a) The capturing behavior of the sea anemone with tentacle cluster. (b) The capturing behavior of the drosera. (c) Folded leaves of the mimosa with anisotropic stiffness.

Another key problem is the mathematical modeling for collisions, especially in the case where soft structures are involved. Previous soft robotic grippers were usually designed to grasp static or quasi-static targets, so their mathematical model mainly focused on static situations [25]. Yang *et al.* presented a virtual work-based static model to describe the deformation and mechanics of continuum robots with a generic rod-driven structure [26]. Kang *et al.* presented a dynamic model for a hyper-redundant tentacle robot using parallel mechanism theory and Newton's law [27]. However, these models did not consider the collision process, so they cannot be used to analyze the soft capture of dynamic targets.

In this paper, we present a novel soft gripper with multiple tentacles and anisotropic stiffness that can capture dynamic targets. The contributions of this work include the following aspects. Firstly, the use of a bio-inspired tentacle cluster can achieve large tolerance to the position and incident angle of the dynamic target without accurate identification of its trajectory, posture and shape. Secondly, the soft bodies of the tentacles help to dissipate and absorb the kinetic energy on impact. Finally, the implementation of anisotropic stiffness in the tentacles can passively block high-speed targets, making it easy for the targets to enter, but difficult to escape the gripper. Finally, a mathematic model to describe the collision dynamics of a tentacle is established and validated experimentally. The presented soft gripper provides a new solution for capturing dynamic targets.

II. Materials and Methods

A. Bio-inspired structure design

When examining existing robotic grippers, error tolerance and grasping force are two major limitations to capture dynamic targets. Inspired by biological structures from animals and plants, we propose the concept of a tentacle cluster to achieve high adaptability to position and orientation errors with the implementation of stiffness anisotropy to passively enhance strength without losing compliance. The presented gripper is like a trap, making it easy for dynamic targets to enter but difficult for them to escape. The gripper consists of multiple flexible tentacles fixed to a rigid base, as shown in **Fig.** 2.

The tentacles are distributed on a circle, forming a 'trap' for the dynamic targets coming from any direction. Each tentacle is composed of an elastic layer on its ventral side and discrete limiting blocks on its dorsal side, as shown in **Fig.** 2(a). This structure enables the tentacle to bend in only one direction, from the dorsal to ventral side, similar to the unidirectional movement of the Mimosas leaves. The limiting blocks are fabricated with resin (Somos® Ledo 6060) material with an elastic modulus of 2600MPa through 3D printing. These blocks are glued to the elastic layer in series with the help of the concave and convex points. The elastic layer is fabricated with polyurethane rubber with an elastic modulus of 50MPa [28], providing the "soft" feature to the gripper [29]. The deformation will occur at the gap between those limiting blocks, which is similar to the flexural hinge in a compliant mechanism [30]. In our case, the elastic layer is 200mm in

This article has been accepted for publication in IEEE/ASME Transactions on Mechatronics. This is the author's version which has not been fully edited and content may change prior to final publication. Citation information: DOI 10.1109/TMECH.2022.3219108

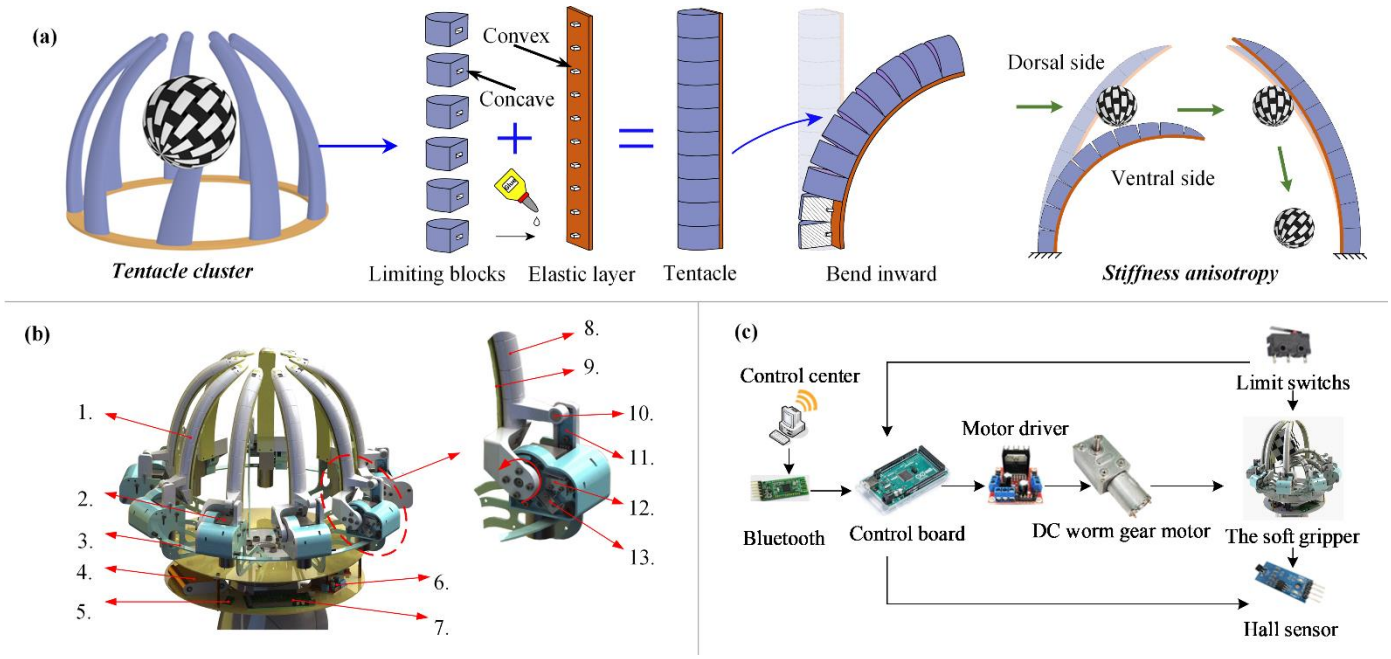

Fig. 2. Prototype of the robotic soft gripper. (a) the concept of the tentacle cluster with stiffness anisotropy and its fabrication process. (b) The soft gripper includes nine modular stiffness-anisotropic tentacles individually attached to the base. 1. Flexible tentacles, 2. DC worm gear motor, 3. Base, 4. Power supply, 5. Bluetooth module, 6. Motor driver, 7. Control board, 8. Limiting block, 9. Elastic layer, 10. Magnet, 11. Hall sensor, 12. Limit switch 1#, 13. Limit switch 2#. (c) Control system of the soft gripper.

length, 24mm in width and 2mm in thickness. The tentacle will bend inward when a dynamic target hits its dorsal side (i.e., outer side of the gripper), allowing the target to enter the gripper, because the tentacle has relatively low stiffness on this side. If the dynamic target keeps moving and hits the ventral side of another tentacle, the tentacle will hold its position and prevent the target from escaping because the bending stiffness on the ventral side is relatively large. Eventually, the target will lose its momentum in the collision process, and fall into the gripper.

Based on the design concept, a prototype of the robotic soft gripper was constructed, as shown in **Fig.** 2(b). The soft gripper includes nine modular flexible tentacles which are individually attached to DC worm gear motors mounted on a base. The motors allow the tentacles to actively rotate about the base. This active rotating motion has two functions: (1) making the tentacles able to bend inward when facing dynamic targets with low speed; (2) allowing for active control of the tentacles to grasp targets.

The control system of the soft gripper is presented in **Fig.** 2(c). The control center sends the task commands (such as waiting for the target, releasing the target etc.) to the control board through a Bluetooth module. The control board takes the task commands, as well as the sensor feedback, and then generates the motor commands for the tentacles. A Hall sensor is mounted on the DC worm gear motor and used to detect the vibration of the flexible tentacle when it is hit by a dynamic target. The limit switches provide the extreme positions for each motor to ensure a safe rotation range.

B. Modeling of the Tentacle

The flexible tentacle cluster will bend inward after being impacted by the dynamic target. The deflection angle of the tentacle is an essential factor to judge whether the target can travel through the tentacle and be captured, so it is necessary to develop a mathematical model for the collision-bending process, based on the information in **Fig.** 3(a). Because all tentacles have identical structure, in the model we take a pair of tentacles to analyze the dynamic relationship between the initial velocity of the target and the deflection of the tentacles.

It is assumed that the center of mass of the tentacle is located in the middle of the elastic layer and the elastic layer will bend with constant curvature [31], as shown in **Fig.** 3(b). The variables contained in the model are summarized in Table I.

TABLE I
NOMENCLATURE

Symbol	Description
$v_{a0'}$, $v_{b0'}$	The velocity component of v_{a0} and v_{b0}
$v_{a'}$, $v_{b'}$	The component velocities of the dynamic target and the center of mass of the left tentacle after a collision
v_a, v_b	The resultant velocities of the dynamic target and the center of mass of the tentacle
P	The distance between the collision point C and the origin O
r_s	The distance between the center of mass of the tentacle A and the origin O
θ	The end deflection angle of the tentacle
T	The kinetic energy of the tentacle
V	The potential energy of the tentacle
Q_k^*	The generalized damping force
x_b, y_b	The position of the center of mass of the left tentacle
x_1	The displacement of target during the collision with the right tentacle
x_2	The displacement of the tentacle tip during the collision
F_1	The impact force acting on the tentacle
k	The equivalent contact stiffness of the tentacle at the collision point D
l	The distance between the collision point D and the tentacle base B

This article has been accepted for publication in IEEE/ASME Transactions on Mechatronics. This is the author's version which has not been fully edited and content may change prior to final publication. Citation information: DOI 10.1109/TMECH.2022.3219108

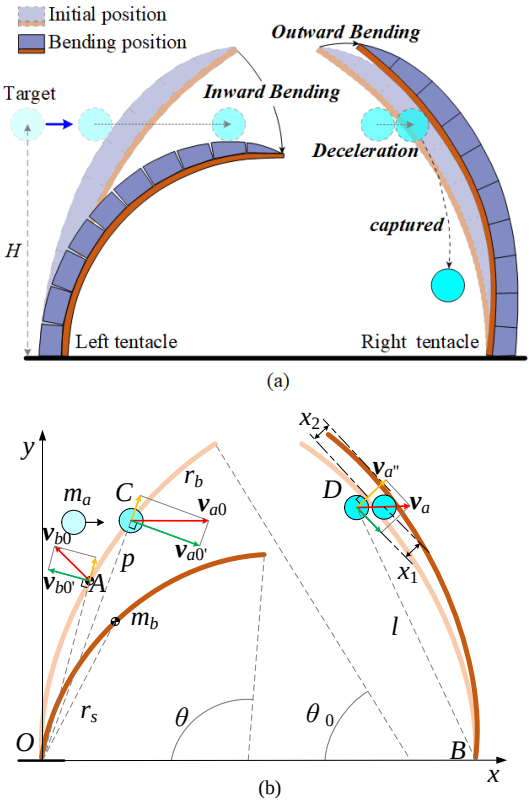

Fig. 3. Modeling and analysis of the flexible tentacles. (a) Initial position before colliding and bending position after colliding. (b) Computational model of the tentacles.

A coordinate system O - xy is attached to the base of the left tentacle, where O is the origin, x and y indicate the horizontal and vertical direction, respectively. When the target collides with the dorsal side of the left tentacle, the angular momentum conservation formula for the left tentacle/target system is

$$m_a \boldsymbol{v}_{a0'} p + m_b \boldsymbol{v}_{b0'} r_s = m_a \boldsymbol{v}_{a'} p + m_b \boldsymbol{v}_{b'} r_s \tag{1}$$

where m_a is the mass of the dynamic target. m_b is the mass of the tentacle. p is the distance between the collision point C and the origin O. r_s is the distance between the center of mass of the tentacle A and the origin O. v_{a0} is the initial velocity of the dynamic target. $v_{a0'}$ is the velocity component of v_{a0} which is perpendicular to the direction of OC. v_{b0} is the initial velocity of the center of mass of the tentacle. $v_{b0'}$ is the velocity component of v_{b0} which is perpendicular to the direction of OA.

The component velocities of the left tentacle and the dynamic target are obtained by applying Newton's hypothesis of kinematic restitution which specifies the ratio of pre- and post-impact velocities as [32]

$$e = \frac{\boldsymbol{v}_{b'} - \boldsymbol{v}_{a'}}{\boldsymbol{v}_{a0'} - \boldsymbol{v}_{b0'}} \tag{2}$$

So, the component velocities of the dynamic target and the center of mass of the left tentacle after a collision are

$$\boldsymbol{v}_{a'} = \boldsymbol{v}_{a0'} - (1+e)\frac{m_b r_s (\boldsymbol{v}_{a0'} - \boldsymbol{v}_{b0'})}{m_a p + m_b r_s} \tag{3}$$

$$\boldsymbol{v}_{b'} = \boldsymbol{v}_{b0'} + (1+e)\frac{m_a p (\boldsymbol{v}_{a0'} - \boldsymbol{v}_{b0'})}{m_a p + m_b r_s} \tag{4}$$

where $r_s = \frac{\sqrt{2} r_b}{\theta}\sqrt{1-\cos\frac{\theta}{2}}$. Here r_b is the total length of the tentacle. Then, the resultant velocities of the dynamic target and the center of mass of the tentacle are

$$\boldsymbol{v}_a = \boldsymbol{v}_{a0} - \boldsymbol{v}_{a0'} + \boldsymbol{v}_{a'} \tag{5}$$

$$\boldsymbol{v}_b = \boldsymbol{v}_{b0} - \boldsymbol{v}_{b0'} + \boldsymbol{v}_{b'} \tag{6}$$

After collision, the left tentacle will bend inward. At this stage, as shown in **Fig.** 3(b), assuming the end deflection angle is θ, the kinetic energy of the tentacle is

$$T = \frac{1}{2} m_b \left(r_s \frac{\dot{\theta}}{4} \right)^2 = \frac{m_b r_b^2 \dot{\theta}^2}{16\theta^2}\left(1-\cos\frac{\theta}{2}\right) \tag{7}$$

The potential energy of the tentacle is

$$V = \frac{E_v I_v}{2 r_b}\theta^2 \tag{8}$$

where $E_v I_v$ is the flexural stiffness of the elastic layer on the ventral side of the tentacle.

During the bending deformation, the left tentacle has internal damping that dissipates the impact energy. Assuming the damping coefficient is c, the generalized damping force is

$$Q_k^* = -c\dot{\theta} \tag{9}$$

Substituting (7) (8) and (9) into Lagranges equation yields

$$\frac{\mathrm{d}}{\mathrm{d}t}\left(\frac{\partial T}{\partial \dot{\theta}}\right) - \frac{\partial T}{\partial \theta} + \frac{\partial V}{\partial \theta} = Q_k^* \tag{10}$$

The dynamic equation of the tentacle is then obtained as

$$\frac{m_b r_b^2}{8\theta^2}\left(1-\cos\frac{\theta}{2}\right)\left(\ddot{\theta} - \frac{\dot{\theta}^2}{\theta}\right) + \frac{m_b r_b^2 \dot{\theta}^2}{32\theta^2}\sin\frac{\theta}{2} + \frac{E_v I_v}{r_b}\theta + c\dot{\theta} = 0 \tag{11}$$

The position of the center of mass of the left tentacle can be obtained as

$$x_b = \frac{r_b}{\theta}\left(1-\cos\frac{\theta}{2}\right) \tag{12}$$

$$y_b = \frac{r_b}{\theta}\sin\frac{\theta}{2} \tag{13}$$

When the target travels through the left tentacle and collides with the right one, the limiting blocks on the right tentacle are squeezed. Because the limiting blocks have high elastic modulus, the deflection of the right tentacle in the outward direction is small. In this collision process, the target will be decelerated rapidly and fall into the gripper, as shown in **Fig.** 3(b). Assuming that the target hits a cantilever beam (the right tentacle) and is stopped, the collision dynamics of the right tentacle/target system can be obtained as

$$\begin{cases} m_a \ddot{x}_1 + \boldsymbol{F}_1 = 0 \\ m_b \ddot{x}_2 - \boldsymbol{F}_1 = 0 \\ x_1(0) = 0, \dot{x}_1(0) = v_{a''} \\ x_2(0) = 0, \dot{x}_2(0) = 0 \end{cases} \tag{14}$$

where $v_{a''}$ is the velocity component of the initial velocity v_a of the target, x_1 is the displacement of target during the collision with the right tentacle, and x_2 is the displacement of the tentacle tip during the collision.

The impact force acting on the tentacle is

This article has been accepted for publication in IEEE/ASME Transactions on Mechatronics. This is the author's version which has not been fully edited and content may change prior to final publication. Citation information: DOI 10.1109/TMECH.2022.3219108

$$\boldsymbol{F}_1(x_1) = kx_1 \tag{15}$$

where k is the equivalent contact stiffness of the tentacle at the collision point D

$$k = \frac{3E_dI_d}{l^3} \tag{16}$$

E_dI_d is the flexural stiffness of the limiting blocks on the dorsal side of the tentacle, and l is the distance between the collision point D and the tentacle base B.

As already mentioned, the deflection angle of the left tentacle is a key factor for the target to get into the gripper. The deflection angle θ of the left tentacle during the collision process can be obtained by solving equations (1) to (13) numerically. The parameters used for the collision simulation are listed in Table II, where the ball has a mass of 50g, radius of 10mm, and an initial velocity of 1.5m/s. It hits the tentacle horizontally with a height H = 120mm from the base at time instant 0.02s. **Fig.** 4 shows the maximum deflection angle (the vertex of the curve, denoted by a '★' symbol) of the tentacle decreases from 174.5° to 112.6° when the elastic modulus of the elastic layer gradually increases from E_v = 30MPa to E_v = 90MPa. According to the Euler-Bernoulli beam theory, the elastic modulus of the elastic layer ≥ 30MPa is enough to ensure that the whole tentacle can maintain its initial position without buckling due to its self-weight in our case. However, the elastic modulus should not be too large in case the dynamic target cannot pass the tentacle and enter into the gripper after collision. For these reasons, we eventually selected a polyurethane rubber material with an elastic modulus of 50MPa for the elastic layer of the tentacle.

TABLE II
LIST OF KEY SIMULATION PARAMETERS IN COLLISION REACTION

Symbol	Description	Value
m_a	Mass of ball	50 g
m_b	Mass of the tentacle	40 g
v_{a0}	Initial velocity of ball	1.5 m/s
v_{b0}	Initial velocity of the center of mass of the tentacle	0
H	Ball hits the tentacle horizontally with a height	120 mm
θ_0	Initial deflection angle of the tentacle	60 deg
e	The restitution coefficient of Newton's hypothesis	0.86
r_b	Total length of the tentacle	200 mm
E_v	The elastic modulus of the elastic layer	From 30 MPa to 90 MPa
Iv	Second moment of area of the elastic layer on the ventral side of the tentacle	192 mm^4
c	Damping coefficient of the polyurethane rubber	15 N·s/rad
E_d	The elastic modulus of the limiting blocks	From 0.5 GPa to 3 GPa
I_d	Second moment of area of the limiting blocks on the dorsal side of the tentacle	1.4×10^5 mm^4

The deceleration effect of the right tentacle is also important for the gripper to stop the target. The deceleration process can be obtained by solving equations (14) to (16) numerically. **Fig.** 5 shows the time required to reduce the velocity component of the target, $v_{a''}$, when the elastic modulus of the limiting blocks increases from E_d = 0.5Gpa to E_d = 3Gpa. A low-cost resin (E_d = 2600Mpa), commonly used in 3D printing machine, was selected to fabricate the limiting blocks in our prototype.

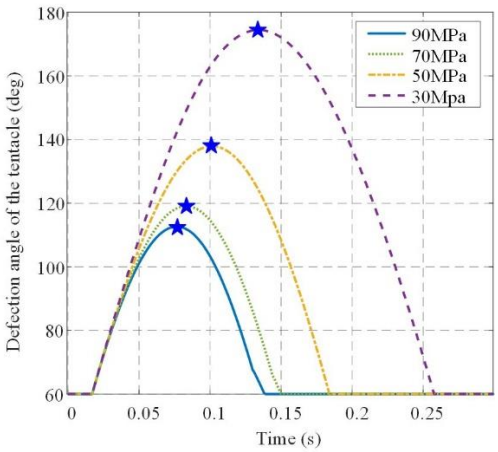

Fig. 4. The calculated deflection angle of the left tentacle after collision.

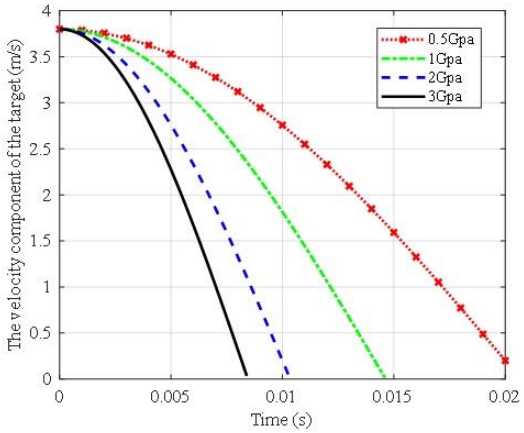

Fig. 5. The simulated results of the target velocity component after collision with the right tentacle.

A successful capture means the target travels through the left tentacle and then is blocked by the right tentacle. We next investigated how the mass and initial velocity of the dynamic target would affect the success rate of the capture via simulation. **Fig.** 6 shows that only if the values of the mass and initial velocity of the dynamic target are within the region on the right side of the dotted line, can the target bend the tentacle enough to travel through and be successfully captured by the soft gripper. A video is also attached to demonstrate this process. The color change from dark blue to red indicates the maximum deflection angle of the tentacle after collision increases from 60° to 240°. It is found that, in the region of success capture (the right side of the dotted line), the tentacle will bend with a maximum deflection angle greater than 120°. The above results are obtained by considering only the passive deflection of the tentacle after a collision. If active control of the tentacle is provided with the help of the DC motors, the requirements for the target mass or initial velocity can be further reduced.

This article has been accepted for publication in IEEE/ASME Transactions on Mechatronics. This is the author's version which has not been fully edited and content may change prior to final publication. Citation information: DOI 10.1109/TMECH.2022.3219108

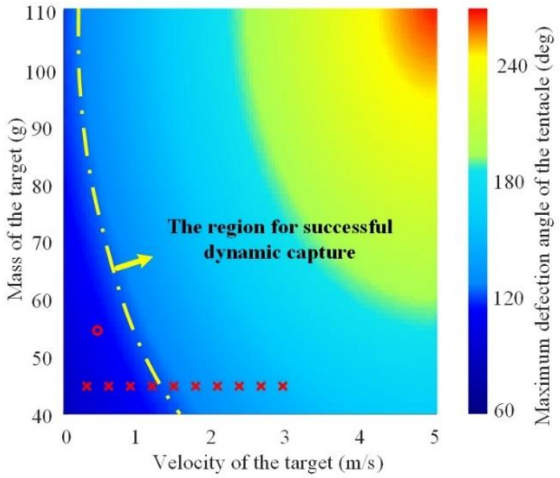

Fig. 6. The region of success capture with respect to the mass and initial velocity of the target.

III. Results

In this section, a series of experiments carried out to assess the performance of the proposed soft gripper are reported. Firstly, the stiffness anisotropy of a single tentacle is demonstrated. Then, a catapult constructed to adjust the launch angle and velocity of the target is described. Throughout the experiments, a high-speed camera was used to record the capturing process. From this, the velocity of the target and deflection angle of the tentacle could be obtained by mapping the image plane to the work plane. In addition, a series of grasping tests were carried out to show that the presented gripper is also able to actively capture static objects with different shapes and masses.

A. Implementation of the Stiffness Anisotropy

An experimental setup to measure the stiffness anisotropy of the tentacle is shown in **Fig.** 7. The tentacle was fixed to a frame at one end, like a cantilever beam. The stiffness of the tentacle was characterized as $k = \boldsymbol{F} / \Delta L$, where $\boldsymbol{F}$ is the loading force in the vertical direction, ΔL is the deflection at the free end. Under an identical loading force $\boldsymbol{F}$ = 2N, the negative deflection ΔL_1 was 3mm while the positive deflection ΔL_2 was 96mm. The force-deflection curves for both ventral and dorsal sides are shown in **Fig.** 7. The stiffness on the ventral side is 34 times greater than that on the dorsal side, which quantifies the anisotropic stiffness in the presented tentacle structure.

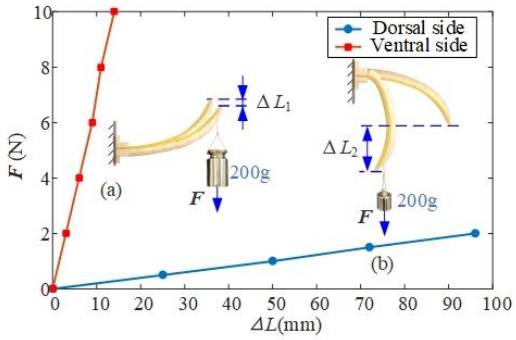

Fig. 7. Comparison of stiffness between the ventral and dorsal sides of the tentacle: (a) Bending under a force in the ventral side. (b) Bending under a force in the dorsal side.

B. Deflection of a Single Tentacle under Impact

To verify the dynamic model of the flexible tentacle presented in **Fig.** 4, a golf ball with a mass of 45g was used as a target. The velocity of the target was increased from 0.3 m/s to 3 m/s in the tests, denoted by the '×' symbols in **Fig.** 6. The maximum deflection angle of the tentacle obtained from simulations and experiments are compared in **Fig.** 6. There is some gap between the simulated and experimental results due to the assumptions in the model of the tentacle (e.g., the location of the center of mass and the uniform curvature). In these tests, the bottom of the tentacle cannot actively rotate inward. The minimum velocity for the golf ball to travel through the tentacle was 1.5m/s and the corresponding maximum deflection angle of the tentacle was 125°. These results also agree with the theoretical results in **Fig.** 8.

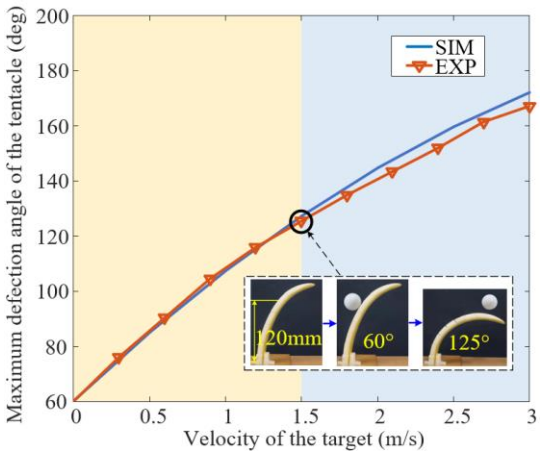

Fig. 8. Simulations and experimental results on the dynamic collision for a single tentacle. The ball will successfully bend the tentacle enough so it will travel through the tentacle when its initial velocity ≥ 1.5m/s and the corresponding maximum deflection angle is 125°.

Figure 9(a) shows that a failure test, denoted by the (○) symbol in **Fig.** 6, which is obtained by only using the passive deflection of the tentacle. A baseball (55g) bounced out of the tentacle because it did not have enough initial velocity. To deal with targets of relatively low velocity, the rotating control for the DC motors at the tentacle bases was utilized. Then, the tentacles could bend inward actively and the baseball successfully fell into the gripper, as shown in **Fig.** 9(b). Such an active rotating strategy can further extend the allowable range of the initial velocity for the targets. A video showing the reduced initial velocity is attached with the paper for reference.

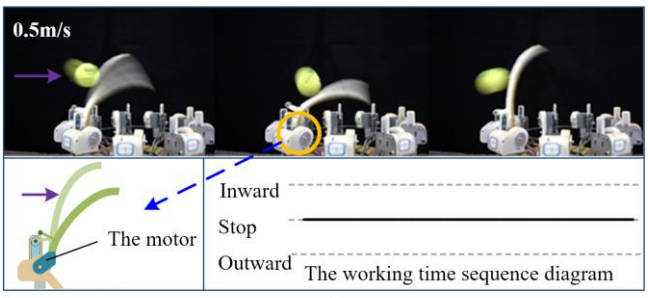

(a)

This article has been accepted for publication in IEEE/ASME Transactions on Mechatronics. This is the author's version which has not been fully edited and content may change prior to final publication. Citation information: DOI 10.1109/TMECH.2022.3219108

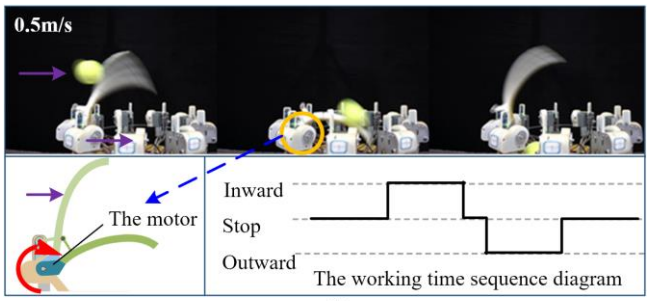

(b)

Fig. 9. The effect of active rotation of the tentacle: (a) With the tentacle rotations disabled, the dynamic target with a velocity of 0.5m/s cannot travel through the tentacle. (b) With the tentacle actively bending inward when the collision happens, the dynamic target with even lower velocity of 0.5m/s can travel through the tentacle.

C. Capture of Targets with Different Incident Angles and Velocities

The next experiment aimed to verify the omni-directional capture capability of the soft gripper for dynamic targets with different velocities. A coordinate system O_1 - x_1y_1 was attached to the center of the base of the tentacle cluster, where O_1 is the origin, and x_1 and y_1 indicate the horizontal and vertical direction, respectively. A cubic box (100g and 100mm) was launched into the soft gripper in a low horizontal direction (the vertical distance from the coordinate origin O_1 was 130mm) with velocity v_1 = 1.5m/s, a high horizontal direction (the vertical distance from the coordinate origin O_1 was 180mm) with velocity v_2 = 2m/s, a diagonally downward direction (incident angle 45°) with velocity v_3 = 1.5m/s, and a vertical direction with velocity v_4 = 1.5 m/s, see **Fig.** 10(a) (1) - (4). As expected, the box falls into the 'trap' in all tests. A video showing these capturing operations is attached with the paper for reference.

The soft gripper thus allows for a wide range of incident angle and velocity to capture the dynamic target, which means there is no need for accurate control for the position and orientation of the gripper. To quantify how the incident angle and velocity of the target affect the capture success rate, we executed the following experiment for a target ball with 10 incident angles (ranging from 0° to 90° with increments of 10°) and 4 initial velocities (1 m/s, 2 m/s, 3 m/s, 4 m/s,). For each combination of incident angle and initial velocity, the test was repeated for 20 times. The number of successful captures is recorded, and the success rate is presented in **Fig.** 10(b).

The experimental results show that the capture success rate was 90% or higher when the incident angle was from 0° to 50° and the velocity over 2 m/s. However, the capture success rate of the soft gripper dramatically decreased as the incident angle increased from 50° to 90° (see **Fig.** 10(b)). The main reason was that the maximum deflection angle of the tentacles was not sufficient for the target to successfully run into the interior of the soft gripper. In summary, the results demonstrate the optimal conditions for the soft gripper to capture dynamic targets, which is 0° to 50° for the incident angle, and more than 2m/s for the target velocity.

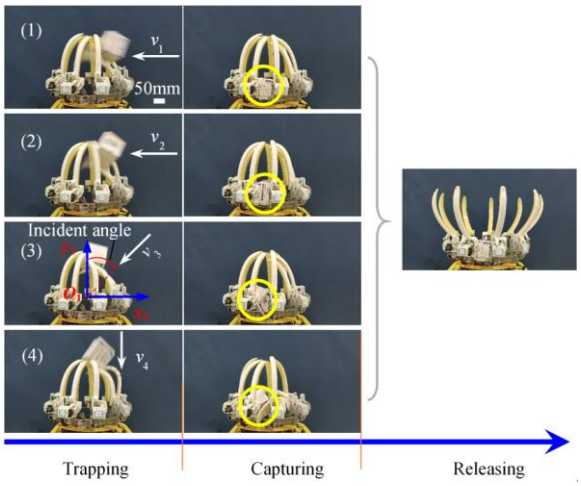

(a)

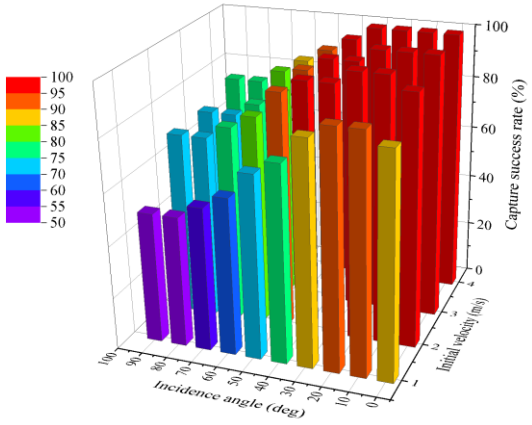

(b)

Fig. 10. The capture of the dynamic target. (a) The target was launched with various velocities and directions, as indicated by the white arrows. The target was released by opening the tentacles in the end. (b) Capture success rate of the soft gripper with respect to the incident angle and initial velocity.

D. Coordination with a Robotic Arm

The performance of the proposed soft gripper was evaluated on a 7-DOF robotic arm, KUKA LBR IIWA. As depicted in **Fig.** 11(a), the target was thrown by a catapult, allowing its flight trajectory to be calculated. In this experiment, the interception position on the trajectory is specified artificially. In practical applications, the trajectory and interception position can be obtained by autonomous devices, but there is no need for accurate calculation and control of them with the help of the presented gripper. The KUKA arm only needs to approximately move the gripper to the interception position, facing to the dynamic target, as shown in **Fig.** 11(b) (1–8). A video is also attached to demonstrate the capture process.

The positioning tolerance of the soft gripper is evaluated as the area where the gripper can be placed to capture the target. As shown in **Fig.** 11(a)(b), a cartesian coordinate system *O'* - *x'y'z'* was attached to the desired interception point O' on the flight trajectory of the target. The *z'* axis was tangent to the flight trajectory. The throw tests for a cube (10mm in side length) were repeated 169 times with the same initial velocity (2m/s) and launch angle (45°). The KUKA arm placed the gripper onto the *x'*-*O'*-*y'* plane, with a constant incident angle of 20° to the z' axis. However, the position of the gripper in

these tests was distributed within a circle about the interception point *O'* (i.e., the origin of the coordinates), as shown in **Fig.** 11(c). The red crosses '×' indicate a successful capture while the blue circles '○' represent failures. It can be seen that the successful capture points are basically distributed within a circle of 150mm in radius. We divided the circle to three concentric parts with interval distance of 50mm. The success rate for each part is shown in **Fig.** 11(d). The higher capture success rate is achieved when the gripper is closer to the desired interception position. Even if the gripper deviated from the desired interception position by 100mm ~ 150mm, the success rate is still 66%. This demonstrates the presented gripper has a high tolerance to the positioning error, which can reduce the complexity of active control.

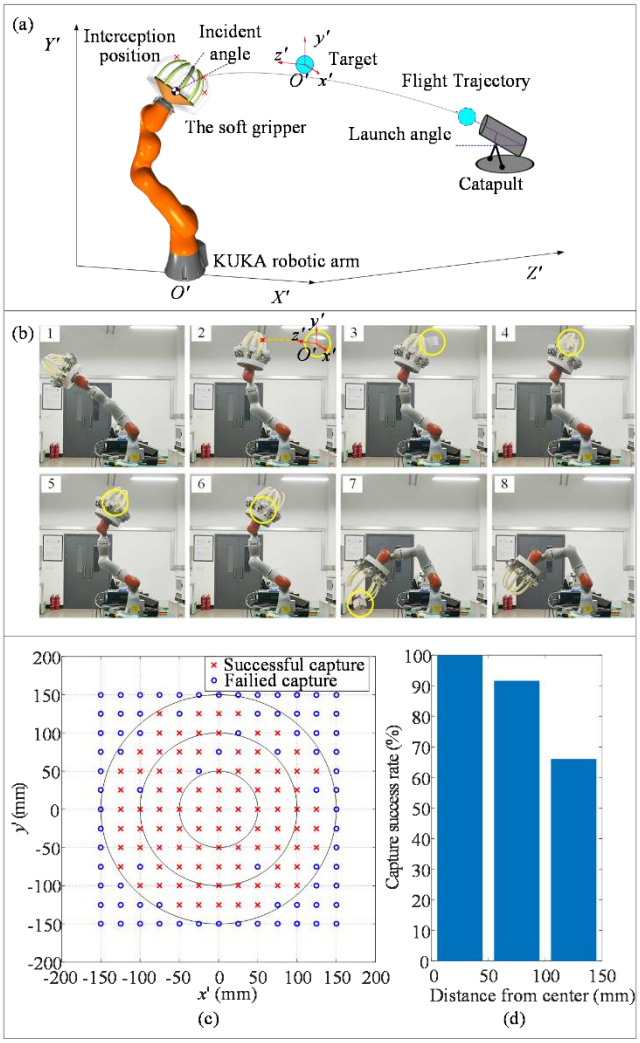

Fig. 11. Coordination with a robotic arm: (a) Experimental set-up for capturing dynamic target. (b) The capturing process: (1–2) the KUKA arm takes the gripper to the interception position; (3) the target, i.e., a cube, hits the gripper; (4–6) the soft gripper captures the dynamic target; (7–8) the gripper releases the target. (c) Capture points of the 169 tests. (d) Variation of the success rate with respect to the distance from the desired interception position.

E. Grasping of Static Target

As mentioned before, the gripper is able to actively rotate its tentacles. So, it can grasp targets moving at very low speed as well as static ones. In another experiment, the adaptability of the soft gripper was confirmed by grasping various static targets with different shapes, sizes, and weights. As shown in **Fig.** 12, the gripper opened its tentacles and moved above the targets. Then, the gripper closed the tentacles to envelop and grasp the targets, such as a ball or another robot. We also show that the soft gripper is able to grasp some special structure on a target much larger than the gripper itself (e.g., grasp the thrust nozzle on a satellite). Release operations are achieved by re-opening the tentacles. A video showing the grasping operations is attached with the paper for reference.

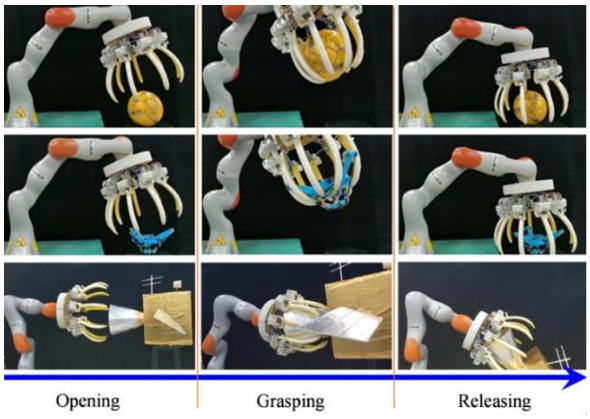

Fig. 12. Sample items grasped by the developed robotic soft gripper. From top to bottom: a soccer ball (0.45kg), a robot (0.8kg), a large target (2.1kg).

IV. Conclusion

This paper presents a novel bio-inspired soft robotic gripper capture mechanism using a tentacle cluster configuration featuring anisotropic stiffness structure for each tentacle.

Due to the unique mechanical design, the presented gripper does not require precise prediction of the target trajectory, nor precise position and orientation control of itself. It is able to capture targets with a large tolerance to their shapes, sizes, incident directions (0° to 50°), velocities (over 2m/s) and positions (achieving 90% success rate even if the actual interception position deviates from the desired one by 100mm). The use of rotating base motors to each tentacle further improves the capability of capturing low-speed as well as static targets.

An analytical model for the tentacle structure is established to describe its bending deformation during the collision. The simulated results generally match the experimental results, which verifies the efficacy of the dynamic model of the tentacles.

The proposed methods pave a new way to design and analyze soft robots for use in collection or removal of dynamic targets in unconstructed environments. Future work will expand the single tentacle analytical model into a multi-tentacle model and implement the gripper/arm system on a moving vehicle to increase the maneuverability of the system.

Acknowledgements

This work was supported by the Natural Science Foundation of China (Grant No. 51875393), and the National Key R&D Program of China (Grant No. 2018YFB1304600 and

2019YFB1309800).

REFERENCES

[1] A. Billard and D. Kragic, "Trends and challenges in robot manipulation," *Science*, vol. 364, no. 1, p. eaat8414, 2019.

[2] K. M. Lynch and M. T. Mason, "Dynamic nonprehensile manipulation: Controllability, planning, and experiments," *Int J Rob Res.*, vol. 18, no. 1, pp. 64-92, 1999.

[3] Y. B. Jia, M. Gardner and X. Mu, "Batting an in-flight object to the target," *Int J Rob Res.*, vol. 38, no. 4, pp. 451-485, 2019.

[4] H. Suzuki and M. Minami, "Visual servoing to catch fish using global/local GA search," *IEEE-ASME Trans. Mechatron.*, vol. 10, no. 3, pp. 352-357, 2005.

[5] Y. Imai, A. Namiki and K. Hashimoto, *et al.*, "Dynamic active catching using a high-speed multifingered hand and a high-speed vision system," *in Proc. IEEE Int. Conf. Robot. Autom.*, 2004, pp. 1849-1854.

[6] S. Kim and A. Billard, "Estimating the non-linear dynamics of free-flying objects," *Rob Auton Syst.*, vol. 60, no. 9, pp. 1108-1122, 2012.

[7] N. Marturi, M. Kopicki and A. Rastegarpanah, *et al.*, "Dynamic grasp and trajectory planning for moving objects," *Auton Robots.* Vol. 43, no. 5, pp. 1241-1256, 2019.

[8] S. Kim, A. Shukla and A. Billard, "Catching objects in flight," *IEEE Trans Robot.*, vol. 30, no. 5, pp. 1049-1065, 2014.

[9] S. S. M. Salehian, M. Khoramshahi and A. Billard "A dynamical system approach for softly catching a flying object: Theory and experiment," *IEEE Trans Robot.*, vol. 32, no. 2, pp.462-471, 2016.

[10] O. White, J. L. Thonnard and A. M. Wing, *et al.*, "Grip force regulates hand impedance to optimize object stability in high impact loads," *Neuroscience.* vol. 189, no. 1, pp. 269-276, 2011.

[11] A. Bhaskar, S. Dantu, S. Roy, J. Lee, S. Baldi, "Adaptive Artificial Time Delay Control for Bipedal Walking with Robustification to State-dependent Constraint Forces," *in Proc. IEEE Int. Conf. adv. Robot.*, 2021, pp. 410-415."

[12] S. Roy, S. B. Roy, J. Lee, S. Baldi, "Overcoming the underestimation and overestimation problems in adaptive sliding mode control," *IEEE-ASME Trans. Mechatron.*, vol. 24, no. 5, pp. 1-1, 2019.

[13] L. Cao, A. T. Dolovich, A. L. Schwab, J. L. Herder and W. Zhang, "Toward a unified design approach for both compliant mechanisms and rigid-body mechanisms: Module optimization," *J. Mech. Des.*, vol. 137, no. 12, pp. 122301, 2015.

[14] J. Y. Wang, C. C. Lan, "A constant-force compliant gripper for handling objects of various sizes," *J. Mech. Des.*, vol. 136, no. 7, pp. 071008, 2014.

[15] L. U. Odhner, L. P. Jentoft and M. R. Claffee, *et al.*, "A compliant, underactuated hand for robust manipulation," *Int J Rob Res.*, vol. 33, no. 5, pp. 736-752, 2014.

[16] N. R. Sinatra, C. B. Teeple and D. M. Vogt, *et al.*, "Ultragentle manipulation of delicate structures using a soft robotic gripper," *Sci Robot.*, vol. 4, no. 33, 2019.

[17] C. Tawk, A. Gillett, M. in het Panhuis, G. M. Spinks and G. Alici, "A 3D-printed omni-purpose soft gripper," *IEEE Trans Robot.*, vol. 35 no. 5, pp. 1268-1275, 2019.

[18] J. Kim, W. Y. Choi and S. Kang, *et al.*, "Continuously variable stiffness mechanism using nonuniform patterns on coaxial tubes for continuum microsurgical robot," *IEEE Trans Robot.*, vol. 35, no. 6, pp. 1475-1487, 2019.

[19] B. Fang, F. Sun and L. Wu, *et al.*, "Multimode Grasping Soft Gripper Achieved by Layer Jamming Structure and Tendon-Driven Mechanism," *Soft Robot.*, 2021.

[20] Y. F. Zhang, N. Zhang and H. Hingorani, *et al.*, "Fast-response, stiffness-tunable soft actuator by hybrid multimaterial 3D printing," *Adv Funct Mater.* Vol. 29, no. 15, pp. 1806698, 2019.

[21] L. Wen, T. Wang and G. Wu, *et al.*, "Quantitative thrust efficiency of a self-propulsive robotic fish: Experimental method and hydrodynamic investigation," *IEEE-ASME Trans. Mechatron.*, vol. 18, no. 3, pp. 1027-1038, 2012.

[22] R. Kang, D. T. Branson and T. Zheng, *et al.*, "Design, modeling and control of a pneumatically actuated manipulator inspired by biological continuum structures," *Bioinspir Biomim.*, vol. 8, no. 3, pp. 036008, 2013.

[23] I. Burgert and P. Fratzl, "Actuation systems in plants as prototypes for bioinspired devices," *Philos Trans A Math Phys Eng Sci*., vol. 367, no. 1893, pp. 1541-1557, 2009.

[24] T. I. Baskin, "Anisotropic expansion of the plant cell wall," *Annu Rev Cell Dev Biol.*, vol. 21, no.1, pp. 203-222, 2005.

[25] Y. Li, Y. Chen and Y. Yang, *et al.*, "Passive particle jamming and its stiffening of soft robotic grippers," *IEEE Trans Robot.*, vol. 33, no. 2, pp. 446-455, 2017.

[26] C. Yang, S. Geng and I. Walker, *et al.*, "Geometric constraint-based modeling and analysis of a novel continuum robot with Shape Memory Alloy initiated variable stiffness," *Int J Rob Res.*, vol, 39, no. 14, pp. 1620-1634, 2020.

[27] R. Kang, D. T. Branson and E. Guglielmino, *et al.*, "Dynamic modeling and control of an octopus inspired multiple continuum arm robot," *Comput Math Appl.*, vol. 64, no. 5, pp. 1004-1016, 2012.

[28] Engineering ToolBox. Young's Modulus, Tensile Strength and Yield Strength Values for some Materials. https://www.engineeringtoolbox.com/young-modulus-d_417.html [Accessed November 29, 2021].

[29] D. Rus and M T. Tolley, "Design, fabrication and control of soft robots," *Nature*, vol. 521, no. 7553, pp. 467-475, 2015.

[30] L. Cao, A. T. Dolovich, A. Chen and W. C. Zhang, "Topology optimization of efficient and strong hybrid compliant mechanisms using a mixed mesh of beams and flexure hinges with strength control," *Mech. Mach. Theory*, vol. 121, pp. 213-227, 2018.

[31] B. A. Jones, I. D. Walker, "Kinematics for multisection continuum robots," *IEEE Trans Robot.*, vol. 22, no. 1, pp. 43-55, 2006.

[32] I. Newton, "Philosophiæ naturalis principia mathematica," (Mathematical principles of natural philosophy). London (1687), 1987.

Shangkui Yang received the B.S. degree in mechanical design manufacturing and automation from the Lanzhou JiaoTong University, Lanzhou, China, and the M.S. degree in mechanical engineering from Northeastern University, Shenyang, China, in 2017 and 2020, respectively. He is currently working toward Ph.D. degree in school of mechanical engineering at Tianjin University, China.

His research interests include robotic design, soft robotics, and continuum robotics.

Yongxiang Zhou received the B.S. degree in mechanical design manufacturing and automation from Northeastern University, Shenyang, China and the M.S. degree in mechanical engineering from Tianjin University, Tianjin, China, in 2018 and 2021, respectively.

His research interests include the design of soft robotics and bio-robots, and robotic dynamics and control.

Ian D. Walker (S'84–M'85–SM'02–F'06) received the B.Sc. degree in Mathematics from the University of Hull, UK, in 1983, and the M.S. and Ph.D. degrees, both in Electrical Engineering, in1985 and 1989, respectively, from the University of Texas at Austin. He has served as Vice President for Financial Activities for the IEEE Robotics and Automation Society, and as Chair of the AIAA Technical Committee on Space Automation and Robotics. He has also served on the Editorial Boards of the IEEE Transactions on Robotics, the IEEE Transactions on

Robotics and Automation, the International Journal of Robotics and Automation, the IEEE Robotics and Automation Magazine, and the International Journal of Environmentally Conscious Design and Manufacturing. He currently serves on the Editorial Board of Soft Robotics. Dr. Walker's research interests include biologically inspired and continuum robotics, as well as architectural robotics.

Chenghao Yang received his bachelor's and master's degrees in mechanical engineering from the Tianjin Polytechnic University, China, in 2014 and 2017, respectively. He is currently a Ph.D. student in school of mechanical engineering, Tianjin University, China.

His research interests include design and control of soft robotics, continuum robotics and medical robotics.

David T. Branson III is Professor of Dynamics and Controls in the Faculty of Engineering – University of Nottingham, UK; director of the Nottingham Advanced Robotics Laboratory, NARLy; and deputy director of the Metrology Manufacturing Team (MMT). He received his undergraduate and master's degrees in mechanical engineering from the University of Wisconsin-Madison, USA, and Ph.D. from the University of Bath, UK. His research interests are in the areas of modelling and control of non-linear systems with application to robotic systems in manufacturing and healthcare environments.

Zhibin Song (Member, IEEE) received the Ph.D. degree in mechanical engineering from the Department of Intelligent Mechanical System, Kagawa University, Takamatsu, Japan, in 2012. He is currently an Associate Professor with the School of Mechanical Engineering, Tianjin University, Tianjin, China. His research interests include mechanisms theory, compliant structure, human– robot interaction, rehabilitation robotics, exoskeleton robotics, and biorobotics. He has published more than 40 articles in his areas of research.

Jian S. Dai (S'14–F'17) received the under-graduate and master's degrees in mechanical engineering from Shanghai Jiao Tong University, Shanghai, China, in 1982 and 1984, respectively, and the Ph.D. degree in advanced kinematics, mechanisms, and robotics from the University of Salford, Salford, U.K., in 1993. He has since taken the post-doctoral study and between 1996 and 1997, was working on reconfigurable and dexterous manipulation of origami-cartons at Unilever Research. He was then taking Senior Lecturer position at University of Sunderland and joined King's College London in 1999. He was promoted to Reader in mechanisms and robotics in 2004 and to Professor in mechanisms and robotics in 2007. Since then, he continues to lead research in the field of mechanisms and robotics with many innovative and leading works in computational and theoretical kinematics, screw theory, metamorphic mechanisms and reconfigurable mechanisms, reconfigurable robotics, with various robot developments including Origami robots, healthcare robots, domestic robots, industrial robots, and terrestrial robots.

Professor Dai is the Fellow of Royal Academy of Engineering, Fellow of the IEEE, ASME and IMechE, and has contributed over 500 publications, including three books.

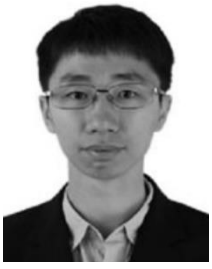

Rongjie Kang received the undergraduate and master's degrees in automation science, and the Ph.D. degree in mechanical engineering from Beihang University, Beijing, China, in 2004, 2006, and 2009, respectively.

He is currently an Associate Professor with the School of Mechanical Engineering, Tianjin University, Tianjin, China. His research interests include continuum robots, bioinspired robots, fluid power control, and mechatronic systems.